# Effect of momentum relaxation on exciton spin dynamics in diluted magnetic semiconductor ZnMnSe/CdSe superlattices

I. A. Buyanova, G. Yu. Rudko, and W. M. Chen
*Department of Physics and Measurement Technology, Linköping University, 581 83 Linköping, Sweden*

K. Kayanuma, A. Murayama, and Y. Oka
*Institute of Multidisciplinary Research for Advanced Materials, Tohoku University, Sendai 980-8577, Japan*

A. A. Toropov, S. V. Sorokin, and S. V. Ivanov
*A. F. Ioffe Physico-Technical Institute, Russian Academy of Sciences, Polytechnicheskaya 26, St. Petersburg 194021, Russia*
(Received 8 November 2004; revised manuscript received 19 January 2005; published 7 April 2005)

cw hot photoluminescence (PL) complemented by transient PL measurements is employed to evaluate momentum and spin relaxation of heavy hole (HH) excitons in ZnMnSe/CdSe superlattices. The rate of acoustic-phonon assisted momentum relaxation is concluded to be comparable to the total rate of exciton decay processes, about $(2-3)\times 10^{10}$ $s^{-1}$, independent of applied magnetic fields. In magnetic fields when the Zeeman splitting $\Delta$ of the exciton states is below the energy of the longitudinal optical (LO) phonon ($\hbar\omega_{LO}$), a surprisingly strong suppression of spin relaxation rate from the bottom of the upper spin band is observed, which becomes comparable to that of momentum scattering via acoustic phonons. On the other hand, dramatic acceleration of the spin relaxation process by more than one order of magnitude is found for the excitons with a high momentum $\boldsymbol{K}$. The findings are interpreted as being due to electron and hole spin flip processes via exchange interaction with isolated $Mn^{2+}$ ions. Experimental evidence for the efficient interaction between the hot excitons and Mn impurities is also provided by the observation of spin flip transitions within $Mn^{2+}$-$Mn^{2+}$ pairs that accompany the momentum relaxation of the hot HH excitons. In higher magnetic fields $\Delta \geqslant \hbar\omega_{LO}$, abrupt shortening of the spin flip time is observed. It indicates involvement of a new and more efficient spin relaxation process and is attributed to direct LO-assisted exciton spin relaxation with a subpicosecond spin relaxation time.

DOI: 10.1103/PhysRevB.71.165203 PACS number(s): 75.50.Pp, 78.20.Ls, 78.55.Et

## INTRODUCTION

A promising trend in semiconductor device evolution lies in addition of spin-dependent functionality to existing principles of operations. Proof-of-principle all-semiconductor spin injection devices have recently been demonstrated,[1–3] where diluted magnetic semiconductors (DMSs) were employed to provide spin-polarized carriers. The success of future spintronic devices requires precise knowledge about ways to create spin-polarized carriers and to control their relaxation dynamics. Spin dynamics of carriers/excitons is often addressed by using time-resolved photoluminescence (PL) spectroscopy, capable of directly measuring spin-flip times.[4–14] However, radiative recombination processes monitored in these studies are most efficient for "cold" excitons/carriers which has zero momentum $\boldsymbol{K}$, to satisfy the momentum conservation requirement. Therefore the main body of experimental information available so far on the spin relaxation is related to $\boldsymbol{K}=0$ excitons. On the other hand, injection of carriers/excitons in spin-functional structures is often accomplished via high energy band states, i.e., with substantial kinetic energy. Spin dynamics under such conditions, even though theoretically predicted to be significantly influenced either by carrier motion[15,16] or by band-mixing effects,[17–20] is rarely addressed experimentally, especially in the case of DMS-based structures.

An alternative approach, which has in the past been successfully used[21,22] to investigate spin-preserving momentum relaxation of excitons in polar semiconductors subject to strong Fröhlich interaction, is the so-called hot PL technique. This technique relies on observation of sharp PL lines from hot excitons which are formed during exciton energy relaxation via cascade emission of longitudinal optical (LO) phonons. Since energy distribution of the hot excitons is determined by the photoexcitation energy, it can therefore be very narrow (determined by a spectral width of a laser). This is in sharp contrast to time-resolved PL measurements which inevitably suffer from a broad spectral width of ultrashort excitation pulses, due to the uncertainty principle. As the energy positions of the hot excitons can be finely tuned by changing the excitation energy, the hot PL approach allows the study of the momentum dependences of various exciton-related processes such as energy transfer, transport of optical excitations, etc. The major drawback of this approach, however, is its incapability of providing exact rates of monitored relaxation processes.

In this work we employ the hot PL technique complemented by time-resolved PL measurements to investigate energy and spin relaxation of hot excitons in ZnMnSe/CdSe superlattices (SLs). Taking full advantage of spin injection device structures only recently available, hot PL arising from nonthermal excitons generated by resonant optical pumping can be greatly enhanced by controlling exciton spin injection from the DMS to an adjacent spin detector (ZnCdSe quantum well in this case). Moreover, the giant Zeeman effect in

 

the DMS ZnMnSe provides a rare possibility of wide-range tuning in the energy separation between exciton spin states by applying an external magnetic field, to the extent even exceeding the LO phonon energy or exciton binding energy—a regime where very little is known about spin-dependent processes in a semiconductor. On the other hand, by tuning excitation photon energy dependence of spin relaxation processes on exciton wave vector $\boldsymbol{K}$ can be assessed.

The paper will be organized as follows. In Sec. II, we shall describe the samples under study and the details of the hot PL and transient PL experiments. In Sec. III, we shall briefly summarize general ideas underlying the hot exciton approach, and shall also highlight new information provided by the approach in a DMS. A detailed account of experimental results on spin-preserving momentum relaxation and decay processes of hot excitons will be presented in Sec. IV. The main body of the paper will be devoted to properties of spin relaxation processes in the investigated structures, including their dependence on exciton kinetic energy and Zeeman splitting of the excitonic states. A discussion of the obtained results will be given in Sec. V, where possible mechanisms for exciton spin relaxation will also be analyzed. Experimental evidence for strong coupling between the hot excitons and magnetic $Mn^{2+}$ ions will be provided in Sec. VI. The main conclusions of the present study will be summarized in Sec. VII.

## II. EXPERIMENTAL

The structures under study were grown by molecular beam epitaxy on a (100) GaAs substrate with a ZnSe buffer layer. They consisted of a ZnMnSe(4 nm)/CdSe(0.8 ML) superlattice (SL) and a 70-Å-thick ZnCdSe quantum well (QW), separated by a ZnSe spacer. The whole structure was cladded between ZnSSe barrier layers to avoid the leakage of carriers from the active regions. The concentration of Mn in the ZnMnSe layers was ~4% which enables a control of the energy distance between the exciton spin subbands undergoing a giant Zeeman splitting of the range of 0–65 meV within the magnetic field range of 0–3 T. The ZnCdSe QW with a lower exciton energy was incorporated in order to provide an effective "sink" for the SL excitons and therefore to ensure the observation of intense hot PL lines related to the SL.

All measurements were carried out in the Faraday configuration in external magnetic fields up to 3 T with the aid of an Oxford split-coil magnet cryostat system. A dye laser tunable in the spectral range of 430–470 nm, was used as an excitation source in cw-PL measurements. The PL signal was dispersed by a Spex 0.85 m double spectrometer and detected by a GaAs photomultiplier. Temperature-dependent PL measurements were carried out in the range of 2–100 K. Time-resolved PL experiments were performed at 4 K. In this case, PL was excited by second-harmonic pulses of a mode-locked Ti:sapphire laser, with a pulse duration of 150 fs and a repetition rate of 80 MHz. The resulting transient PL was recorded by a streak camera system through a spectrometer (with a time resolution of about 15 ps). In all measurements the incident laser beam was linearly polarized unless specified. The circular polarization of the PL was recorded with the aid of a quarter wave retardation plate and a linear polarizer. PL polarization degree is defined in percentage by $P=100(\sigma^+-\sigma^-)/(\sigma^++\sigma^-)$.

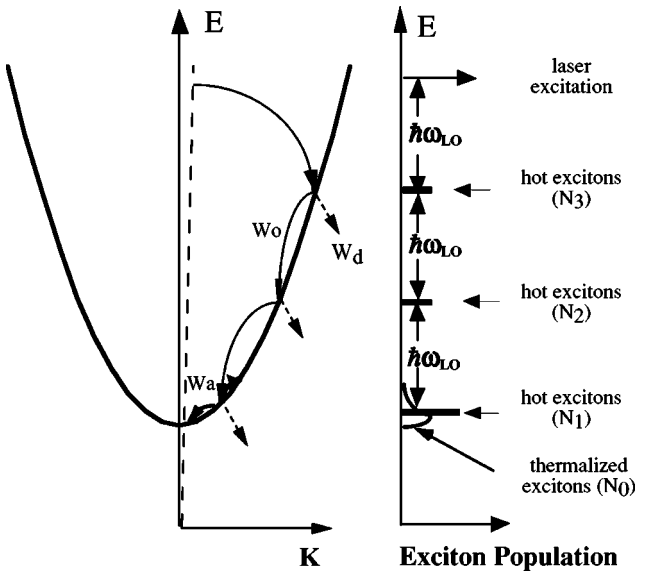


FIG. 1. In the left panel a schematic illustration of various relaxation processes within an exciton band are shown by solid arrows, such as a fast exciton cascade involving emission of optical phonons $W_0$ and slower momentum relaxation assisted by acoustic phonons $W_a$. The latter process becomes important at the bottom of the excitonic branch. Exiton (photon) dispersion $E(K)$ is shown by the solid (dashed) line. Dashed arrows $W_d$ illustrate all decay processes from the exciton state. In the right panel, exciton populations at various energies following a monochromatic optical excitation are shown. Narrow peaks ("levels") in the exciton distribution are created due to the fast energy relaxation via emission of the LO phonons (denoted as $N_m$ where $m \geqslant 1$ is counted from the bottom of the exciton state). Population of the thermalized excitons ($N_0$) at the bottom of the exciton branch is established via interactions with acoustic phonons.

## III. HOT EXCITON RELAXATION: APPROACH

Hot exciton spectroscopy is known to be a valuable tool for tackling various energy relaxation processes in semiconductors. Below we will briefly summarize general ideas underlying the hot exciton approach, and will highlight new information which becomes accessible in DMS.

### A. B=0

Absorption of excitation light with energy higher than the forbidden energy gap can create as an immediate result large-momentum excitons, by simultaneous emission of one LO phonon (Fig. 1). Kinetic energy distribution of the excitons is then established as a result of a balance between various energy relaxation processes including emission of acoustic and optical phonons and exciton decay, as discussed in detail in Ref. 21. For II-VI semiconductors with strong Fröhlich interaction, the energy relaxation of the hot excitons pre-

dominantly occurs via emission of LO phonons. This is due to a high ($\sim 10^{12}$–$10^{13}$ $s^{-1}$) probability of the LO-assisted energy relaxation ($W_0$), which dominates over all other processes. This relaxation process creates population of the hot excitons at energies ("levels") that are displaced from the excitation photon energy ($\hbar\omega_{opt}$) by an integer number of LO-phonon energy ($\hbar\omega_{LO}$)—Fig. 1. At zero magnetic field, the hot exciton distribution can be obtained from the following rate equations:[21]

$$dN_m/dt = G_{opt} - N_m(W_d + W_0), \tag{1}$$

$$dN_{m-1}/dt = N_m W_0 - N_{m-1}(W_d + W_0), \tag{2}$$

$$dN_1/dt = N_2 W_0 - N_1(W_d + W_a), \tag{3}$$

where $G_{opt}$ is the optical generation rate, $N_m$ is the population of the quasilevel $m$ (counting from the bottom of the exciton branch), $W_0$ is the probability of the LO-assisted energy relaxation, $W_d$ is the probability of all decay processes from the exciton branch including exciton dissociation, recombination (both radiative and nonradiative) and trapping. In our structures a new process, i.e., exciton escape from the DMS SL to the QW through the ZnSe spacer, is introduced and should be included in $W_d$. Interactions of the hot excitons at the bottom of the band with acoustic phonons will eventually result in equilibrium (or thermalized) exciton population $N_0$:

$$dN_0/dt = N_1 W_a - N_0 W_d. \tag{4}$$

In a steady-state condition, all quasilevels have been shown[21] to have a comparable population of hot excitons except for the one at the bottom of the excitonic band $N_1$ which has much higher exciton density—Fig. 1. Moreover, the ratio between the population of thermalized and hot excitons at the bottom of excitonic band is determined from Eq. (4) by the probabilities of acoustic phonon relaxation and exciton decay:

$$\frac{N_1}{N_0} = \frac{W_d}{W_a}. \tag{5a}$$

The exciton distribution can be experimentally monitored by measuring light emission from the corresponding states. Radiative recombination of the thermalized excitons will lead to a broad PL band, whereas emissions of the hot excitons are seen as a series of hot PL lines displaced by an integer number of LO-phonon energy from the excitation photon energy. Strictly speaking, the emission of 2 LO phonons is required for the hot PL observation, to satisfy momentum conservation. However, in systems with a high degree of disorder this requirement becomes softened and the 1-LO hot PL line is often seen.[21,23,24]

In-depth analysis of the hot PL allows one to evaluate probabilities of various relaxation processes in the investigated samples. For example, observation of the hot PL lines evidences that the rate of the exciton relaxation via emitting LO phonons is higher than that for the exciton decay. Furthermore, relative intensities of the thermalized exciton emission ($I_0$) and the last (i.e., close to the bottom of the excitonic branch) hot PL line ($I_1$) reflect relative importance

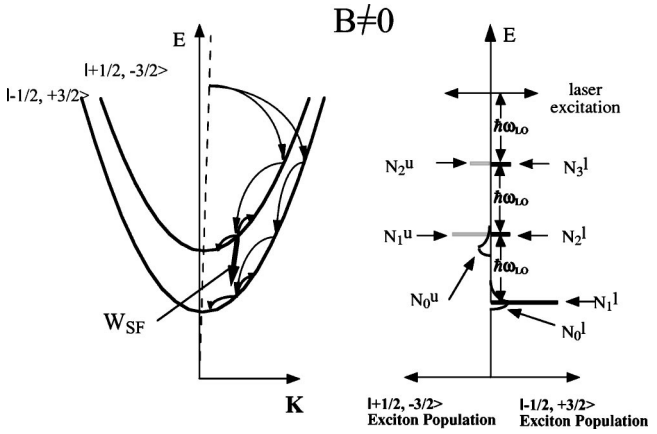


FIG. 2. Exciton dispersion and energy relaxation processes in an applied magnetic field $B$ (the left part of the figure). For simplicity, only the optically active exciton states of the heavy hole exction are shown. In addition to spin-conserving momentum relaxation processes as illustrated in Fig. 1, interband spin-flip transitions between the two exciton branches become important (shown by the thick solid arrow). The right side of the figure shows the population distributions of the two exciton states in the presence of magnetic fields.

of the acoustic-phonon assisted momentum relaxation and the exciton decay. As the later can be directly measured from the PL transient studies, efficiency of momentum relaxation via emission of acoustic phonons can be easily determined. Naturally, excitons can also be created as a result of free carrier absorption. In this case thermalization of photocreated carriers can precede their binding into the exciton. Such process will increase the population of the thermalized excitons, enhancing intensity of the corresponding PL. Therefore, the equality (5a) should be replaced by the inequality

$$\frac{I_1}{I_0} \leqslant \frac{W_d}{W_a}, \tag{5b}$$

where $I_0$ and $I_1$ are experimentally measured intensities of the thermalized and the last hot PL line, respectively.

### B. B ≠ 0

Information on exciton spin relaxation can be obtained by analyzing the hot PL properties in an applied magnetic field. Indeed, a magnetic field lifts spin degeneracy of exciton states, which results in a splitting $\Delta$ of the exciton branches, as shown schematically in Fig. 2 for the heavy-hole (HH) exciton in ZnMnSe. (For simplicity, only optically active HH exciton states are shown.) Under optical excitation with linearly polarized light, both spin-split excitonic states become populated. Subsequent energy relaxation of the hot excitons can occur via phonon-assisted intraband scattering preserving spin orientation of the excitons or via interband spin-flip transitions between the two exciton branches. Contributions of spin relaxation processes should become more important for the excitons near the bottom of the upper spin-split branch. This is because the spin-flip transitions between the two exciton branches at high $\boldsymbol{K}$, which may accompany fast

LO-assisted momentum relaxation,[6] will partly cancel each other. Therefore the populations of the spin-split exciton states under applied magnetic fields become

$$dN_0^l/dt = N_1^l W_a + N_0^u W_{\mathrm{SF}}^- - N_0^l W_d - N_0^l W_{\mathrm{SF}}^+,$$

$$dN_0^u/dt = N_1^u W_a - N_0^u W_{\mathrm{SF}}^- - N_0^u W_d + N_0^l W_{\mathrm{SF}}^+, \qquad (6)$$

where the subscript $u(l)$ denotes the upper (lower) exciton state. $W_{\mathrm{SF}}^{\pm}$ is the rate of spin flip transition from the corresponding state:[16]

$$W_{\mathrm{SF}}^{\pm} = \frac{1}{\tau_{\mathrm{SF}}[1+\exp(\pm\Delta/k_B T)]}. \qquad (7)$$

Here $\tau_{\mathrm{SF}}$ denotes the spin relaxation time and $k_B$ is the Boltzmann constant $W_{\mathrm{SF}}^+$ is negligible for $\Delta \gg k_B T$, i.e., for a range of magnetic fields used in the present study. This simplifies Eq. (6) such that under the steady state condition

$$\frac{I_1^u}{I_0^u} = \frac{W_d^u + W_{\mathrm{SF}}^-}{W_a}. \qquad (8)$$

Evidently, relative intensities of the thermalized and hot exciton PL from the upper spin state critically depend on the spin relaxation rate. This enables us to evaluate efficiency of this process as a function of energy spacing $\Delta$ between the spin-split exciton states (e.g., by varying applied magnetic fields), and also its dependence on exciton wave vector $\boldsymbol{K}$ (e.g., by tuning excitation photon energy).

## IV. SPIN-CONSERVING MOMENTUM RELAXATION OF HOT EXCITONS

A representative PL spectrum of the ZnMnSe/CdSe SL is shown in Fig 3(a). It consists of a broad band and sharp lines, arising from the radiative recombination of the excitons from the HH-exciton branch in the DMS SL. The broad band, of which the line shape is independent of the excitation energy, corresponds to the recombination of the excitons that are thermalized at the bottom of the exciton band. The corresponding transition can be independently monitored by measuring PL excitation spectra of the adjacent nonmagnetic QW, where the observation of the HH DMS exction reflects exciton injection from the DMS to the QW (Ref. 25)—Fig. 3(b). On the other hand, the sharp emission lines are displaced from the excitation photon energy by an integer number of LO phonon energy of 31.6 meV. All sharp lines have comparable intensities with the exception of the one at the lowest energy which exhibits strong enhancement in resonance with the ground state of the HH excitons—shown by dots in Fig. 3(a). At zero magnetic field, the sharp lines (and also the broad emission) are unpolarized independent of the polarization of the excitation light. This is illustrated in Fig. 4 for the 1LO feature under linearly polarized excitation. We interpret these transitions as being due to the hot excitons PL which appears as a result of the hot exciton relaxation cascade via multiple loss of the LO-phonon energy.[23,24] An alternative explanation for the sharp lines as being due to multi-phonon resonant Raman scattering can be ruled out

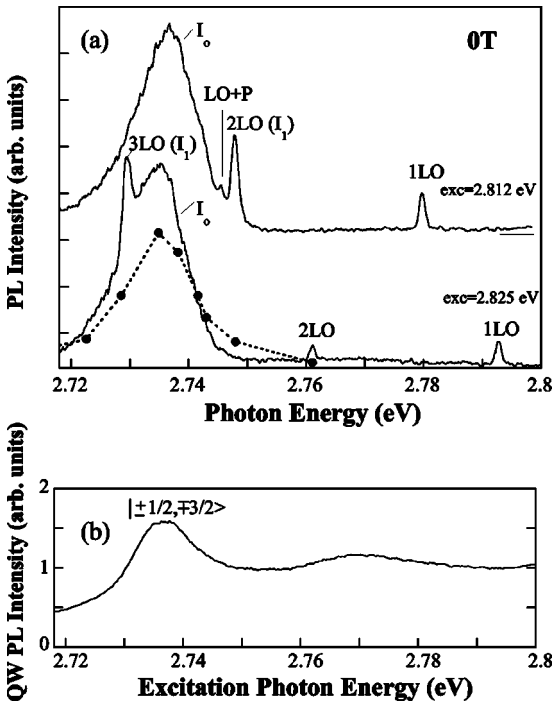


FIG. 3. (a) Typical photoluminescence spectra of the HH exciton in the ZnMnSe/CdSe DMS SL measured at 2 K in zero magnetic field under optical excitation with the specified photon energies. Spectral dependence of the hot 2LO-line intensity, which exhibits resonant enhancement with the HH exciton, is also shown (dots). (The dashed curve is just a guide for the eye.) (b) Photoluminescence excitation spectrum of the nonmagnetic ZnCdSe QW. The excitonic transition related to the optically active HH exciton in the ZnMnSe/CdSe SL is clearly seen due to exciton injection from the DMS to the QW.

since this coherent process should be correlated with the polarization of the excitation light and therefore will only be allowed in the $x(y,z)\bar{x}$ polarization for the used backscattering geometry from a (100) surface, inconsistent with the experimental data (Fig. 4).

In addition to the LO lines, another sharp feature (denoted as "LO+P") with much weaker intensity at approximately 2.3 meV below the lowest LO transition can be seen in Figs.

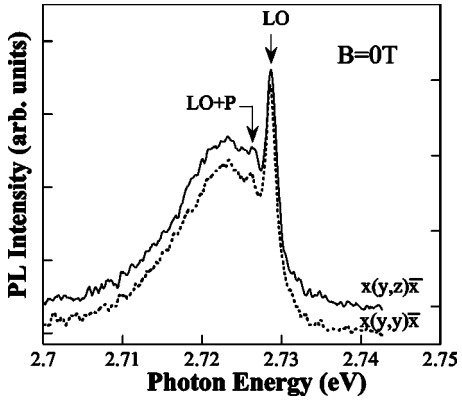


FIG. 4. PL spectra of the DMS SL measured at 2 K with the specified polarizations in the backscattering geometry from the (100) surface.

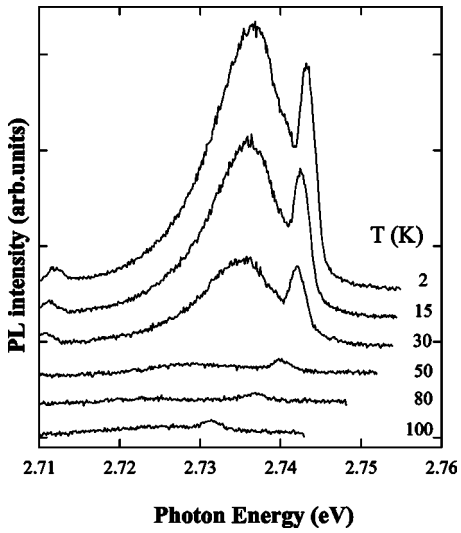


FIG. 5. PL spectra from the DMS SL measured at zero field as a function of measurement temperatures. The excitation photon energy has been shifted at each temperature following the shift of the DMS bandgap.

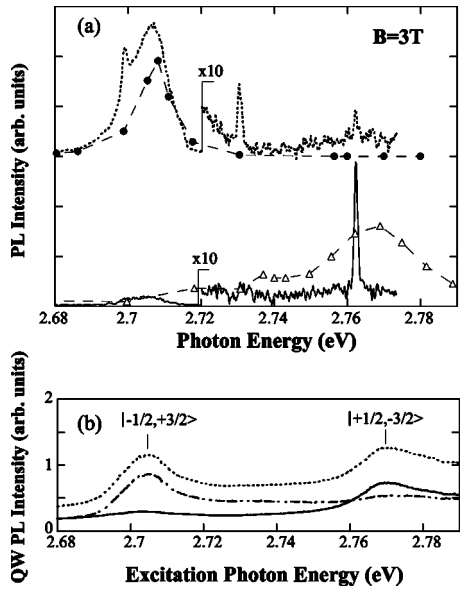


FIG. 6. (a) PL spectra of the HH exciton from the DMS SL measured at 3 T with the $\sigma^+$ (dashed line) and $\sigma^-$ (solid line) polarizations. The PL was excited by using linearly polarized light at 2.793 eV that provides excitation of both spin-split exciton branches. Dots (open triangles) are intensities of the 2LO hot PL detected in the $\sigma^+$ ($\sigma^-$) polarization. (b) Photoluminescence excitation spectra of the nonmagnetic QW measured under the linear (dashed line), $\sigma^+$ (dashed-doted line), and $\sigma^-$ (solid line) excitations. Transitions related to the $|-1/2,+3/2\rangle$ and $|+1/2,-3/2\rangle$ states of the HH exciton can only be excited in the $\sigma^+$ and $\sigma^-$ polarizations, respectively, as expected from the selection rules.

3 and 4. The properties of the LO+P line closely resemble that of the hot PL transitions, such as similar dependence on the excitation photon energy and polarization indicating that it is related to some inelastic scattering process accompanying kinetic energy relaxation of the hot excitons. Physical origin of this process will be discussed in detail in Sec. VI.

The observation of the LO-lines of hot PL [Fig. 3(a)] provides evidence that the rate of the exciton relaxation via emitting LO phonons ($W_0$) is higher than the total rate of other decay processes of the excitons within the SL ($W_d$). Moreover, the observed similar intensity for the thermalized and hot PL is indicative for comparable rates of the acoustic phonon-assisted momentum relaxation ($W_a$) and other decay processes ($W_d$). The lifetime of the HH excitons was determined to be $\tau_d \sim 30$ ps by time-resolved PL. This provides the low bound for the acoustic phonon relaxation time $\tau_a = 1/W_a$ as being $\sim 30-50$ ps, in reasonable agreement with the previously deduced value of 100 ps for ZnSe-based quantum wells.[12]

Increasing temperature caused a rapid decrease in the overall PL intensity. This decrease is, however, more severe for the broad PL band—Fig. 5. The observed behavior can be explained, within the framework of the analysis, by an increasingly important role of nonradiative processes in the exciton decay that is thermally activated more efficiently than the acoustic phonon relaxation.

## V. EXCITON SPIN RELAXATION

Application of a magnetic field lifts the spin degeneracy of the HH excitonic states in the DMS and causes giant Zeeman shifts of the optically active $|-1/2,+3/2\rangle$ and $|+1/2,-3/2\rangle$ states due to strong $s,p$-$d$ interactions with $Mn^{2+}$ ions. Here the notation $|m_e,m_h\rangle$ is used to describe the excitonic states, and $m_e$ and $m_h$ denote the angular momentum projection of the electron and hole, respectively. The splitting of the excitonic states can be closely monitored by measuring the PLE spectra of the nonmagnetic QW. This is demonstrated in Fig. 6(b), where both optically active excitonic transitions are apparent under excitation with linearly polarized light [shown by the dotted line in Fig. 6(b)]. As expected from the selection rules, the lower $|-1/2,+3/2\rangle$ state is $\sigma^+$ active, whereas transitions to the upper $|+1/2,-3/2\rangle$ state acquires the $\sigma^-$ polarization—shown in Fig. 6(b) by the dashed and solid lines, respectively.

In PL experiments, two spin-split excitonic subbands give rise to two sets of the optical transitions with opposite polarization. The optical transition from the bottom of the lowest exciton state gives rise to a strong broad PL band, which undergoes a redshift in an applied magnetic field and exhibits strong $\sigma^+$ polarization (up to 90%)—see Fig. 6(a). Likewise, the same polarization was observed for the hot PL components that are in resonance with the $|-1/2,+3/2\rangle$ state. On the other hand, the hot PL lines resonant with the upper lying $|+1/2,-3/2\rangle$ state are $\sigma^-$ polarized. Spectral dependences of the hot PL components with the $\sigma^+$ and $\sigma^-$ polarizations are shown in Fig. 6(a) by filled and opened symbols, respectively. It is clear that the distribution of the hot excitons has now transformed into two branches when the excitons are accumulated near the bottom of the $|-1/2,+3/2\rangle$ and $|+1/2,-3/2\rangle$ subbands after the hot exciton cascades.

A number of new and interesting features emerge under in-depth investigations of hot excitons in applied magnetic fields. For example, relative intensities of the hot and ther-

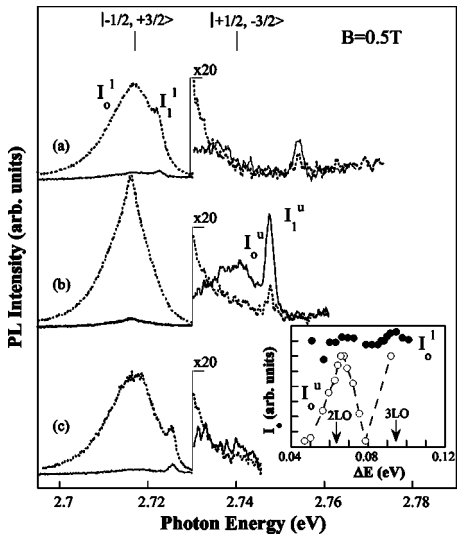


FIG. 7. PL spectra from the HH exciton in the DMS SL measured at 0.5 T with the $\sigma^+$ (dashed line) and $\sigma^-$ (solid line) polarizations as a function of the excitation photon energy. (a), (b), and (c) correspond to the excitation photon energies of 2.818, 2.812, and 2.790 eV, respectively. Also indicated on the top of the figure are the spectral positions of the $|-1/2,+3/2\rangle$ and $|+1/2,-3/2\rangle$ states determined by measuring the PLE spectra of the nonmagnetic QW. The Zeeman splitting of the excitonic states $\Delta$ is equal to 22 meV and is smaller than the LO phonon energy. The inset shows dependences of the thermalized PL components from the lower ($I_0^l$) and upper ($I_0^u$) states as a function of the energy difference $\Delta E$ between the excitation photon energy and the bottom of the corresponding state.

malized PL components related to the upper-lying $|+1/2, -3/2\rangle$ state, which reflect the $N_0^u$ and $N_1^u$ populations, are found to critically depend on the excitation energy and also on an applied magnetic field. We will show below that this behavior reflects surprisingly strong dependence of spin relaxation from the upper exciton state on the wave vector $\boldsymbol{K}$ and spin splitting of the exciton states.

### A. Dependence on the wave vector

Representative PL spectra recorded as a function of excitation photon energy in moderate magnetic fields ($k_BT<\Delta<\hbar\omega_{\mathrm{LO}}$) are shown in Fig. 7. Whereas the intensity $I_0^l$ of the thermalized PL from the lowest $|-1/2,+3/2\rangle$ state is practically independent from the excitation energy, a resonant enhancement of the $I_0^u$ intensity was observed when the excitation photon energy exceeds the energy of the upper exciton state by approximately an integer number $n$ of the LO phonon energy $\hbar\omega_{\mathrm{LO}}$ (to be referred to below as resonant excitation). This effect is demonstrated in Fig. 7, where the appearance of the $\sigma^-$-PL component at 2.74 eV is clearly seen for the excitation energy of 2.812 eV, i.e., about 2 $\hbar\omega_{\mathrm{LO}}$ above the bottom of the $|+1/2,-3/2\rangle$ exciton branch. The dependences of the thermalized PL components from the upper and lower excitonic states on the excitation photon energy are shown in the inset of Fig. 7. The observed PL enhancement provides direct evidence for a dramatic increase in the population of the $|+1/2,-3/2\rangle$ state under the resonant excitation, i.e., when the hot exciton cascade due to the LO-assisted momentum relaxation ends near the bottom of the excitonic band. We would like to point out that the spin splitting between the two excitonic states at 0.5 T, i.e., under the experimental conditions of Fig. 7, is about 23 meV, which exceeds by more than two orders of magnitude the thermal energy at the measurement temperature of 2 K. Assuming a Boltzmann distribution, the spin temperature of excitons is estimated to be up to 85 K, much higher than the lattice temperature, to account for the experimentally observed ratio of $I_0^u/I_0^l \approx 0.02-0.03$.

Let us now discuss possible reasons responsible for the observed strong dependence of the exciton population on the excitation energy. Under the steady state condition, intensity of an optical transition associated with an excitonic state is determined by the product of its generation rate and lifetime. Therefore an increase in intensity of the $|+1/2,-3/2\rangle$ transition under the resonant excitation could reflect either an enhancement in the generation rate to the bottom of the corresponding excitonic branch due to the fast carrier relaxation via emission of LO phonons or an increase of the exciton lifetime. The former should, however, apply to both spin-split states and should lead to a similarly strong dependence of the exciton population on the excitation photon energy if this mechanism dominates. In our studies only minor modifications in the populations of the lower spin band, seen as a week (10–15 %) oscillatory changes of $I_0^l$ with the excitation energy, was observed (shown in the inset in Fig. 7). Consequently, an increase of the generation rate of the exciton state can not be the dominant mechanism responsible for the observed dramatic enhancement (by more than 10 times) in the $I_0^u$ intensity of the upper spin band.

Therefore, the observed strong dependence of $I_0^u$ on the excitation photon energy should be attributed to a substantial change in the exciton lifetime of the $|+1/2,-3/2\rangle$ state, i.e., in the total rate of exciton decay and spin flip processes $W_d^u+W_{\mathrm{SF}}$. It changes from $W_d^u+W_{\mathrm{SF}} \gg W_a$ under "off-resonance" conditions to $W_d^u+W_{\mathrm{SF}} \sim W_a$ under the resonant excitation. In principle, the exciton decay rate could somewhat depend on the energy position of the final step of the LO-assisted hot exciton cascade and thus on the excitation photon energy if it is dominated by the exciton tunneling from the DMS to the nonmagnetic QW. This is because the probability of the tunneling process exponentially depends on the height of the tunneling barrier. The contribution of the tunneling process to the total exciton decay rate in the investigated structures can be estimated by comparing results from the time-resolved PL measurements in the samples with different widths of the tunneling barrier—see Fig. 8. Apparently, an increase in the barrier width by two times does not affect the exciton lifetime. This can only mean that the exciton decay is mainly determined by nonradiative recombination within the DMS, which does not significantly depend on the exciton energy, judging from the minor changes in the intensity of the $|-1/2,+3/2\rangle$ transition—see the inset in Fig. 7.

This leaves a slow down of the spin relaxation rate $W_{\mathrm{SF}}$ of the $|+1/2,-3/2\rangle$ excitons near the bottom of the excitonic branch, i.e., with a small wave vector $\boldsymbol{K}$, as the most plau-

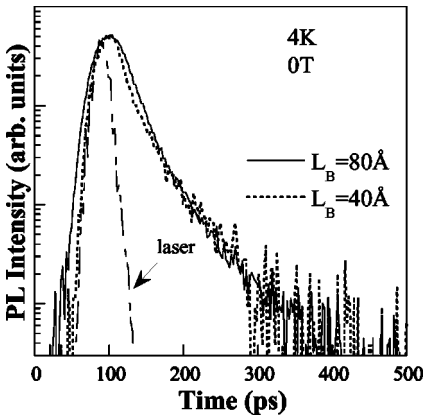


FIG. 8. Normalized PL decays of the HH exciton measured at zero field from the DMS SL structures with two different widths of the tunneling barrier between the SL and nonmagnetic QW. The measurements were performed at 4 K in zero field with the excitation photon energy of 2.851 eV. The measured transient behavior of the laser pulse is also shown by the dashed-dotted line, to demonstrate time response of the system.

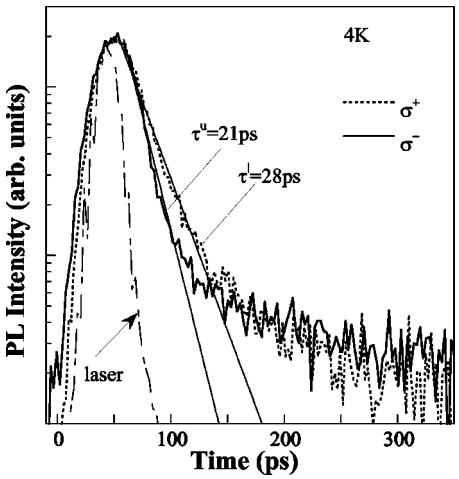


FIG. 9. Decay curves of the normalized integrated PL intensities of the $|+1/2,-3/2\rangle$ (thick solid line) and $|-1/2,+3/2\rangle$ (dashed line) excitonic transitions from the DMS SL measured at 1.0 T. The excitation photon energy was 2.851 eV. The thin solid lines are fitting curves by analyzing rate equations with fitting parameters $\tau_d=28$ ps and $\tau_{\mathrm{SF}}=84$ ps. The measured transient behavior of the laser pulse is also shown by the dashed-dotted line, to demonstrate time response of the system.

sible physical mechanism for the observed resonant enhancement of the corresponding thermalized PL $I_0^u$. From Eq. (6), it can thus be concluded that $W_{\mathrm{SF}}\sim W_a$ under the resonant excitation and $W_{\mathrm{SF}}\gg W_a$ under the off-resonance conditions. In other words, the spin relaxation time for the excitons near the bottom of the upper exciton branch (near $\boldsymbol{K}=0$) should be comparable to the value typical for acoustic phonon relaxation ($\sim$30–50 ps). This leads to an accumulation in the population of the upper spin state, which effectively raises the spin temperature well above that of the lattice. On the other hand, the spin relaxation time for the $\boldsymbol{K}\neq 0$ excitons should be substantially shortened and should fall in the range of 1–3 picoseconds, to assure more than ten times decrease in the $I_0^u$ intensity observed under the off-resonance excitation.

The spin relaxation (or spin-flip) time for the excitons near the bottom of the excitonic branch can be independently and directly determined from transient PL measurements. Representative PL decays measured at 1 T from both spin-split excitonic states are shown in Fig. 9. The effective lifetimes of 21 and 28 ps can be estimated for the upper $|+1/2,-3/2\rangle$ and lower $|-1/2,+3/2\rangle$ excitons, respectively. With the aid of rate equation analysis, this yields the spin-flip time $\tau_{\mathrm{SF}}=84$ ps when the spin splitting $\Delta\approx 18$ meV, assuming that the observed shortening of the exciton lifetime for the $|+1/2,-3/2\rangle$ state as compared with that for the $|-1/2,+3/2\rangle$ state is solely attributed to the spin-flip process, i.e.,

$$\frac{1}{\tau^{u(l)}}=\frac{1}{\tau_d}+\frac{1}{\tau_{\mathrm{SF}}\left[1+\exp\left(\mp\frac{\Delta}{k_BT}\right)\right]}. \tag{9}$$

Here $\tau^{u(l)}$ is the measured exciton lifetime from the corresponding spin-split state, and $\tau_d=1/W_d=28$ ps is the characteristic time for all exciton decay processes (except for the spin-flip transition) deduced from the decay time of the lower spin state. The corresponding fits of the experimentally measured PL decays are shown by the thin solid lines in Fig. 9. The obtained value mainly reflects the spin-flip rate for the excitons near $\boldsymbol{K}=0$, that are allowed to recombine by the momentum conservation law, and is in very good agreement with the results from the cw measurements.

### B. Dependence on the spin splitting between the excitonic states

In order to further examine the physical origin of the spin relaxation processes occurring in the investigated structures, the populations of $\boldsymbol{K}=0$ excitons were studied as a function of Zeeman splitting $\Delta$ of the exciton states. Dependence of the $I_0^u/I_1^u$ ratio measured under the resonant excitation condition is shown by filled dots in Fig. 10(a). The corresponding values of $I_0^u/I_1$ are found to be practically constant for moderate Zeeman splittings, i.e., when $k_BT<\Delta<\hbar\omega_{\mathrm{LO}}$. A constant ratio of the "thermalized" and hot PL intensities implies that the spin-flip rate is independent of $B$, expected for $\Delta\gg k_BT$—see Eq. (9). This behavior is indeed observed in the time-resolved PL experiments, where a constant spin-flip time (dots) of around $90\pm10$ ps is observed when 8 meV $<\Delta<20$ meV—Fig. 10(b). Furthermore, from the characteristic time constants for all relaxation processes measured from the transient studies, the value of $I_0^u/I_1^u$ can be estimated by using Eq. (8). The corresponding results are shown by the dashed-dotted line in Fig. 10(a) and are in very good agreement with the $I_0^u/I_1^u$ values measured in the cw experiments. This proves the credibility of the hot PL approach and also indicates that the exciton spin dynamics in moderate magnetic fields is governed by the same spin relaxation process with a constant spin-flip time.

Also obvious from Fig. 10(a), a further increase of spin splitting with $\Delta$ approaches and exceeds $\hbar\omega_{\mathrm{LO}}$, largely facili-

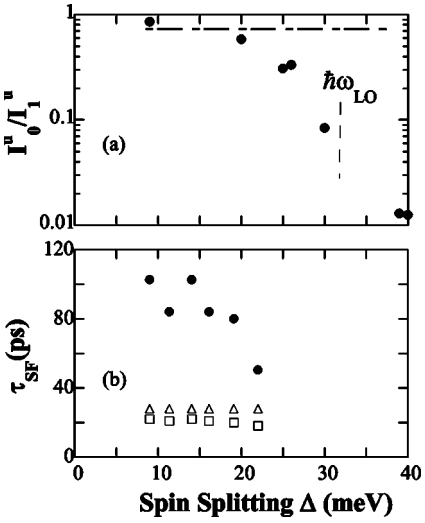


FIG. 10. (a) Experimentally measured ratio (dots) between the thermalized and hot PL intensities from the upper spin state as a function of the Zeeman splitting Δ between the excitonic states. The dashed-dotted line represents values estimated from Eq. (8) assuming the following time constants of the relaxation processes: $\tau_a$ =50 ps, $\tau_d$=28 ps, $\tau_{SF}$=90 ps. The rate of the spin flip process was assumed to be independent of Δ when $\Delta \gg k_B T$ as expected from Eq. (9). (b) PL decay times measured for the upper (open squares) and lower (open triangles) exciton states as a function of the Zeeman splitting Δ of the excitonic states. Dots represent spin relaxation times deduced from the measured decay times according to Eq. (9).

tates exciton spin relaxation, which causes a dramatic quenching of the "thermalized" emission from the $|+1/2, -3/2\rangle$ state. As an example, Fig. 11 shows representative PL spectra recorded in the $\sigma^+$ (dotted lines) and $\sigma^-$ (solid lines) polarizations as a function of excitation photon energies at

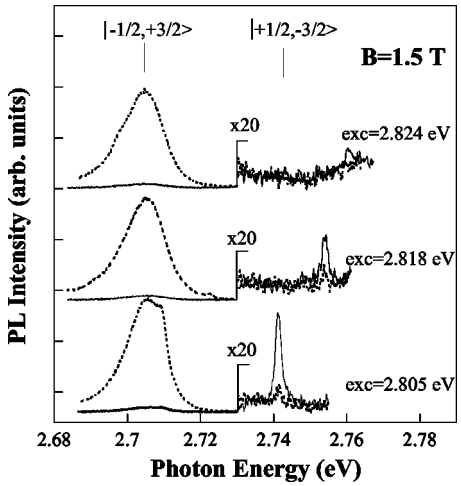


FIG. 11. PL spectra from the HH exciton in the DMS SL measured with the $\sigma^+$ (dashed line) and $\sigma^-$ (solid line) polarizations as a function of excitation photon energy. Also indicated are spectral positions of the $|-1/2, +3/2\rangle$ and $|+1/2, -3/2\rangle$ states determined by measuring the PLE spectra of the nonmagnetic QW. The Zeeman splitting Δ between the excitonic states is equal to 39 meV and exceeds the LO phonon energy.

$B$=1.5 T (Δ=39 meV). Even though the hot PL transitions from the $|+1/2, -3/2\rangle$ state are clearly observed, no "thermalized" emission $I_0{}^u$ from this excitonic state can be detected, in contrast to the results of Fig. 7 for moderate Zeeman splittings. This is indicative for a strong enhancement in the spin relaxation rate with increasing spin splitting, which becomes faster than the spin-conserving acoustic phonon relaxation even under the resonant excitation condition. This is further supported by a shortening of the decay time of the $|+1/2, -3/2\rangle$ transitions from the transient PL measurements, which falls beyond the time resolution of the detection system. (Note that the $\tau_{SF}$ value of 50 ps deduced when Δ=22 meV represents the upper limit for the spin-flip time.) Both hot PL and transient PL results imply that a new spin relaxation process of high efficiency becomes activated when the spin splitting of the excitonic states exceeds the LO energy.

### C. Possible mechanisms

We will now address the physical origin of exciton spin relaxation in the investigated structures. In nonmagnetic quantum structures, the spin relaxation of the HH excitons has been shown[11,16] to be dominated by the long-range *e-h* exchange interaction which gives rise to direct spin relaxation between the $|+1/2, -3/2\rangle$ and $|-1/2, +3/2\rangle$ spin-split states due to simultaneous flips of both electron and hole spins. This interaction weakens linearly with decreasing $\boldsymbol{K}$ and should vanish at $\boldsymbol{K}=0$ resulting in the spin relaxation time in the range of tens to hundreds of picoseconds, taking into account homogenous broadening and dephasing of the exciton state.[16] Even though these properties are in principle consistent with the results presented in Sec. V A, we do not think that the long range *e-h* exchange represents the dominant spin relaxation process for the excitons in the studied structures. This is because such process should be suppressed by magnetic fields applied normal to the quantum well plane, which is opposite to our experimental findings.

Alternatively, the exciton spin flips can occur by subsequent flips of electron or hole spins via the dark exciton states $|+1/2, +3/2\rangle$ and $|-1/2, -3/2\rangle$. Possible spin relaxation mechanisms for single carriers which exhibit strong momentum dependence include the Elliot-Yafet[17,18] and D'yakonov-Perel[15] mechanisms, both mediated via the spin-orbit interaction. According to the Elliot-Yafet mechanism, spin-orbit interaction causes mixing of electron wave functions with opposite spin orientations, which couples momentum scattering with spin depolarization. However, the efficiency of this mechanism should decrease with increasing bandgap energy, which makes it less probable as compared to other mechanisms present in ZnMnSe. In the case of the D'yakonov-Perel scattering, the spin flip is assured by lifting spin degeneracy of the conduction band states in a crystal that lacks inversion symmetry. Due to the energy dependence of the conduction band splitting, the efficiency of this mechanism substantially enhances with increasing kinetic energy (and therefore momentum $\boldsymbol{K}$) but should be suppressed by an external magnetic field, inconsistent with our experimental results.

Another spin relaxation process theoretically predicted[20,26] to be very efficient in DMS-based quantum structures is the strong $s,p$-$d$ exchange interaction with magnetic ions. In this case the spin flips of electrons and holes are facilitated by simultaneous spin flips of $Mn^{2+}$ ions. We will argue below that an interplay of electron and hole spin flips via this interaction can explain the experimentally observed properties of exciton spin relaxation in moderate magnetic fields (i.e., when the Zeeman splitting of the excitonic states is below the LO phonon energy). We therefore suggest it as the dominant mechanism responsible for the exciton spin relaxation under these conditions. Indeed, the corresponding spin-flip relaxation times of holes are largely $\boldsymbol{K}$ dependent.[20] This is because these transitions require mixing of the heavy-hole and light hole states, prohibited near $\boldsymbol{K}=0$ by a large energy separation between the corresponding states (i.e., around 30 meV in our structures due to combined effects of quantum confinement and strain). Admixture of the LH character with increasing $\boldsymbol{K}$ therefore results in dramatic acceleration of the hole spin relaxation with a characteristic time within a picosecond or even subpicosecond range. Therefore, increasing $\boldsymbol{K}$ should promote hole spin flip transitions leading to an overall increase of the exciton spin-relaxation rate. The proposed mechanism is also consistent with the observed insensitivity of the exciton spin relaxation to applied magnetic fields when $\Delta < \hbar\omega_{\mathrm{LO}}$. We need to point out that the measured spin-flip time in our structures is more than one order of magnitude shorter than that deduced for the strained ZnMnSe epilayers.[7] This is probably not surprising as the exchange interaction with magnetic ions is of very short ranges and therefore critically depend on the overlap between the wavefunctions of the excitons/carriers and magnetic ions, i.e., predicted to be by far more efficient in quantum structures.[20,26]

As was mentioned above, an increase of magnetic fields above $\Delta \geqslant h\omega_{\mathrm{LO}}$ leads to a dramatic increase of the spin relaxation rate, which becomes more than one order of magnitude faster than the rate of acoustic phonon relaxation even for the $\boldsymbol{K}=0$ excitons. This indicates the involvement of a new spin relaxation process of high efficiency which becomes activated when the Zeeman splitting of the exciton states approaches the LO energy. The corresponding process was previously assigned to a direct LO-assisted exciton spin relaxation[27] when the exciton spin flips and the phonon emission occur as a result of a single quantum transition. Taking advantage of both hot PL and time-resolved spectroscopies, we can now provide an estimate of the characteristic spin relaxation time for this process to be shorter than 1–3 ps, judging from the ratio of the "thermalized" and hot PL intensities related to the upper exciton state.

## VI. EXCITON SCATTERING BY MAGNETIC IONS

Efficient interactions between $Mn^{2+}$ ions and the excitons in the investigated structures are directly evident from the observation of an additional feature (denoted as "LO+P" in Figs. 3 and 4) that is displaced from the hot PL line by approximately 2.3 meV. The energy loss during this scattering process accompanies the LO-assisted kinetic energy relaxation of the hot excitons. It does not depend on applied magnetic fields, evident from the same energy spacing between the LO and LO+P transitions independent of $B$—see Fig. 12. This indicates that it cannot be caused by spin scattering of a 3$d$ electron bound to an isolated $Mn^{2+}$ ion as the Zeeman splitting $g_{\mathrm{Mn}}\mu_B B$ of its $S_{5/2}$ ground state is proportional to $B$, where $g_{\mathrm{Mn}}=2$ is the $g$ factor of the electron localized at $Mn^{2+}$. On the other hand, it is well known that Mn ions, when present at high concentrations, tend to form nearest-neighbor pairs coupled antiferromagnetically. An effective spin Hamiltonian for the $Mn^{2+}$-$Mn^{2+}$ pair can be written as

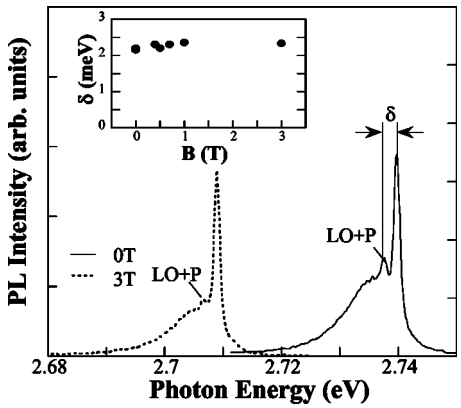


FIG. 12. PL spectra from the HH exciton in the DMS SL measured at 0 T (solid line) and 3 T (dashed line), respectively. The insert shows the energy separation $\delta$ between the LO and LO+P lines as a function of an applied magnetic field $B$.

$$H = -J[S(S+1) - 35/2] + g_{\mathrm{Mn}}\mu_B MB, \tag{10}$$

where $J$ is the constant of $Mn^{2+}$-$Mn^{2+}$ exchange interaction, $\boldsymbol{S}=\boldsymbol{S}_1+\boldsymbol{S}_2$ is the total effective spin of the Mn-Mn pair with $S=0,1,\ldots,5$. $M=-S,\ldots,+S$ is the projection of the spin angular momentum of the $Mn^{2+}$ ion along the direction of $B$. The zero field splitting between the ground ($S=0$) and the first excited ($S=1$) states of the pair is $|\delta E|=2J=2.1-2.2$ meV, if we use the value $J=12.25-12.8$ K found for ZnMnSe-based quantum structures.[28,29] The obtained value is in excellent agreement with the energy separation between the LO+P and LO transitions, showing that it reflects the energy transferred from the exciton to the $Mn^{2+}$-$Mn^{2+}$ pair. The observed independence of this energy on applied magnetic field further supports this conclusion. Indeed, even though the magnetic field lifts degeneracy of the spin triplet excited state of the pair, only $\Delta M=0$ transitions, of which the energy does not change with $B$, are optically allowed according to the selection rules. On the other hand, the splitting of the $S=1$ triplet state should result in a decrease in the intensity of the LO+P line in applied magnetic fields as only one of the three spin states contributes to the LO+P transition, in agreement with our experimental observation—Fig. 12. Therefore we attribute the LO+P line to be a result of the exciton scattering via a transition between the spin states of a Mn pair which accompanies the LO-assisted momentum relaxation of the HH exciton. The appearance of this line in the PL spectra provides direct ex-

perimental evidence for the involvement of magnetic ions in the exciton relaxation. Naturally, one would also expect observation of the spin flip transitions related to the isolated $Mn^{2+}$ ions with substantially higher concentrations. However, due to a small energy loss during this process, which is about 0.35 meV for $B=3$ T, the corresponding transitions can not be resolved within the linewidth ($\sim$1.5 meV) of the dominant LO-assisted transition.

## VII. CONCLUSIONS

In summary, we have employed the hot exciton approach complemented with the transient PL measurements to evaluate momentum and spin relaxation of the HH excitons in the ZnMnSe/CdSe SL. Based on the analysis of the relative intensities of the thermalized and hot PL lines the rate of acoustic-phonon assisted momentum relaxation is found to be comparable to the total rate of exciton decay processes, i.e., around $2-3\times10^{10}$ $s^{-1}$, independent of applied magnetic fields.

A close examination of the hot exciton PL in applied magnetic fields provided evidence for the presence of two different mechanisms for the exciton spin relaxation, with their relative importance being critically dependent on the Zeeman splitting of the exciton states. In magnetic fields $\Delta<\hbar\omega_{\mathrm{LO}}$, the exciton spin relaxation is found to depend critically on the exciton momentum but is not affected by magnetic fields. Specifically, a surprisingly strong suppression of spin relaxation from the bottom (i.e., when $\boldsymbol{K}=0$) of the upper-lying $|+1/2,-3/2\rangle$ spin band is observed, which becomes comparable to momentum scattering via acoustic phonons. This conclusion was independently verified from the time-resolved PL measurements, which yield the spin relaxation time of 90 ps for $\boldsymbol{K}=0$ excitons, i.e., of the same order as the energy relaxation time due to spin-conserving acoustic phonon scattering. On the other hand, dramatic acceleration of the spin relaxation is found for the excitons with a high momentum leading to the spin relaxation time in the range of a few ps. The observed findings are interpreted as being due to electron and hole spin flip processes via the strong exchange interaction with isolated $Mn^{2+}$ ions. Experimental evidence for the efficient interaction between the hot excitons and Mn impurities is also provided from the observation of the spin flip transitions within $Mn^{2+}$-$Mn^{2+}$ pairs which accompany the momentum relaxation of the HH excitons.

In higher magnetic fields $\Delta\geqslant\hbar\omega_{\mathrm{LO}}$, the observed abrupt shortening of the spin flip time indicates the involvement of the new spin relaxation process of high efficiency, which is tentatively attributed to a direct LO-assisted exciton spin relaxation when the change of the exciton spin and the phonon emission occurs as a result of a single quantum transition. The characteristic spin relaxation time for this process is estimated to be shorter than 1–3 ps for the $\boldsymbol{K}=0$ excitons.

## ACKNOWLEDGMENTS

The financial support by the Swedish Research Council, the Wenner-Gren Foundation, and the Swedish Foundation for International Cooperation in Research and Higher Education is greatly appreciated. We are grateful to Dr. I. G. Ivanov for his expert assistance with the dye laser.

[1] R. Fiederling, M. Keim, G. Reuscher, W. Ossau, G. Schmidt, A. Waag A, and L. W. Molenkamp, Nature (London) **402**, 87 (1999).
[2] Y. Ohno, D. K. Young, B. Beschoten, F. Matsukura, H. Ohno, and D. D. Awschalom, Nature (London) **402**, 790 (1999).
[3] M. Oestreich, J. Hübner, D. Hägele, P. J. Klar, W. Heimbrodt, W. W. Rühle, D. E. Ashenford, and B. Lunn, Appl. Phys. Lett. **74**, 1251 (1999).
[4] J. F. Smyth, D. A. Tulchinsky, D. D. Awschalom, N. Samarth, H. Luo, and J. K. Furdyna, Phys. Rev. Lett. **71**, 601 (1993).
[5] W. C. Chou, A. Petrou, J. Warnock, and B. T. Jonker, Phys. Rev. B **46**, 4316 (1992).
[6] D. A. Tulchinsky, J. J. Baumberg, D. D. Awschalom, N. Samarth, H. Luo, and J. K. Furdyna, Phys. Rev. B **50**, 10 851 (1994).
[7] C. D. Poweleit, A. R. Hodges, T.-B. Sun, L. M. Smith, and B. T. Jonker, Phys. Rev. B **59**, 7610 (1999).
[8] T. C. Damen, K. Leo, J. Shan, and J. E. Cunningham, Appl. Phys. Lett. **58**, 1902 (1991).
[9] L. Munoz, E. Perez, L. Vina, and K. Ploog, Phys. Rev. B **51**, 4247 (1995).
[10] B. Baylac, T. Armand, M. Brousseau, X. Marie, B. Dareys, G. Bacquet, J. Barrau, and R. Planet, Semicond. Sci. Technol. **10**, 295 (1995).
[11] R. Spiegel, G. Bacher, A. Forchel, B. Jobst, D. Hommel, and G. Landwehr, Phys. Rev. B **55**, 9866 (1997).
[12] M. Umlauff, J. Hoffmann, H. Kalt, W. Langnbein, J. M. Hvam, M. Scholl, J. Söllner, M. Heuken, B. Jobst, and D. Hommel, Phys. Rev. B **57**, 1390 (1998).
[13] A. Filoramo, R. Ferreira, Ph. Roussignol, R. Planel, and V. Thierry-Mieg, Phys. Rev. B **58**, 4617 (1998).
[14] J. Urdanivia, F. Iikawa, M. Z. Maialle, J. A. Brum, P. Hawrylak, and Z. Wasilewski, Phys. Rev. B **65**, 115336 (2002).
[15] M. I. D'yakonov and V. I. Perel', Sov. Phys. JETP **33**, 1053 (1971); Sov. Phys. Solid State **13**, 3023 (1972).
[16] M. Z. Maiulle, E. A. de Andrade e Silva, and L. J. Sham, Phys. Rev. B **47**, 15 776 (1993).
[17] R. J. Elliott, Phys. Rev. **96**, 266 (1954).
[18] Y. Yafet, in *Solid State Physics*, edited by F. Seitz and D. Turnbull (Academic, New York, 1963), Vol. 14.
[19] T. Uenoyama and L. J. Sham, Phys. Rev. Lett. **64**, 3070 (1990).
[20] R. Ferreira and G. Bastard, Phys. Rev. B **43**, 9687 (1991).
[21] For a review, see, e.g., S. Permogorov, Phys. Status Solidi B **68**, 9 (1975).
[22] G. Fasol, W. Hackenberg, H. P. Hughes, K. Ploog, E. Bauser, H. Kano, Phys. Rev. B **41**, 1461 (1990).
[23] D. Some and A. V. Nurmikko, Phys. Rev. B **48**, 4418 (1993).
[24] A. A. Toropov, T. V. Shubina, A. V. Lebedev, S. V. Sorokin, S. V. Ivanov, G. R. Pozina, J. P. Bergman, and B. Monemar, J. Cryst. Growth **214/215**, 806 (2000).
[25] I. A. Buyanova, I. G. Ivanov, B. Monemar, W. M. Chen, A. A.

Toropov, Ya. V. Terent'ev, S. V. Sorokin, A. V. Lebedev, S. V. Ivanov, and P. S. Kop'ev, Appl. Phys. Lett. **81**, 2196 (2002).
[26] G. Bastard and L. L. Chang, Phys. Rev. B **41**, 7899 (1990).
[27] W. M. Chen, I. A. Buyanova, G. Y Rudko, A. G. Mal'shukov, K. A. Chao, A. A. Toropov, Ya. Terent'ev, S. V. Sorokin, A. V. Lebedev, S. V. Ivanov, and P. S. Kop'ev, Phys. Rev. B **67**, 125313 (2003).
[28] J. Puls and F. Henneberger, J. Cryst. Growth **214/215**, 432 (2000).
[29] I. I. Reshina, S. V. Ivanov, D. N. Mirlin, A. A. Toropov, A. Waag, and G. Landwehr, Phys. Rev. B **64**, 035303 (2001).